

## Numerous Polymorphic Phases $\text{BaBi}_3\text{O}_{5.5}$ Related to the Perovskite

F. ABBATTISTA,\* M. HERVIEU,† M. VALLINO,\* C. MICHEL,† AND B. RAVEAU†

\**Dipartimento di Scienza dei Materiali e Ingegneria Chimica, Politecnico di Torino, Turin, Italy,* and †*Laboratoire CRISMAT, CNRS URA 1318, ISMRa Université de Caen, Boulevard du Maréchal Juin, 14050 Caen Cedex, France*

Received June 1, 1992; in revised form September 10, 1992; accepted October 20, 1992

In the binary system  $\text{BaO}-\text{Bi}_2\text{O}_3$ , the composition  $\text{BaBi}_3\text{O}_{5.5}$  was synthesized at three temperatures, 630, 700, and 730°C, and studied by electron diffraction and X-ray diffraction. For the highest temperature, electron diffraction reveals a cubic subcell with *I*-type symmetry ( $a = 4.384 \text{ \AA}$ ) and the existence of an incommensurate modulated structure. For 700°C a monoclinic subcell is observed ( $a = 4.328 \text{ \AA}$ ,  $b = 4.497 \text{ \AA}$ ,  $c = 4.328 \text{ \AA}$ ,  $\beta = 90^\circ 22'$ ) with superstructure corresponding to  $5a \times 4b \times 4c$ . For the lowest temperature, three kinds of cubic crystals coexist:  $a \times a \times a$  with and without incommensurate satellites and  $2a \times 2a \times 2a$ . A model is proposed to explain the *I*-type symmetry in the high temperature sample. © 1993 Academic Press, Inc.

### Introduction

The discovery of the superconductive perovskites  $\text{BaPb}_{1-x}\text{Bi}_x\text{O}_3$  (1) and  $\text{Ba}_{1-x}\text{K}_x\text{BiO}_3$  (2) has drawn attention to the fact that the study of the crystal chemistry of ternary or pseudoternary bismuth oxides is of primary importance for the understanding of superconductivity at high temperature in these materials. In this respect the ternary system  $\text{Bi}-\text{Ba}-\text{O}$  appears very complex and to date is not really understood. The stoichiometric perovskite  $\text{BiBaO}_3$  itself has been the subject of controversy, with various symmetries of the simple cubic perovskite cell being reported by different authors (1, 3–8). The structure of this oxide and its monoclinic symmetry were definitely established by Thornton and Jacobson (9). More recently Chaillout *et al.* (10) performed a systematic neutron diffraction study of  $\text{BaBiO}_3$  on 11 differently prepared samples. This showed the existence of two structural arrangements due to order–disorder phe-

nomena of Bi (III) and Bi (V) in two independent crystallographic sites. From the investigation of the phase diagram of the system  $\text{BaO}-\text{Bi}_2\text{O}_3$ , Krstanovic and co-workers (11) showed the existence of a wide homogeneity range of the perovskite structure on the bismuth-rich side. In order to shed some light on this issue we have reinvestigated this system. We report here on the synthesis and crystallographic characterization of several forms of  $\text{BaBi}_3\text{O}_{5.5}$  which may be related to the perovskite.

### Experimental

The samples, characterized by an atomic ratio  $\text{Bi}/\text{Ba} = 3/1$ , were prepared starting from  $\text{Bi}_2\text{O}_3$  and  $\text{Ba}(\text{NO}_3)_2$ , both of analytical grade. The two chemical constituents were thoroughly mixed by grinding with acetone in an agate mortar and pestle. After evaporation of the organic solvent the powder was pressed into loose pellets and calcined in air at about 650°C for few hours, in order to

decompose Ba(NO<sub>3</sub>)<sub>2</sub> into BaO. The solid obtained, visibly heterogeneous, was carefully homogenized by regrinding and then pelletized under a pressure of 2 ton/cm<sup>2</sup> into the shape of a cylinder (10 mm in diameter and 6–8 mm in thickness). The pellets were heated at different temperatures ranging from 600 to 750°C in silver vessels, with grinding and repelletizing after each heat treatment. Duration of each heat treatment was never lower than 48 hr.

The evolution of the samples after each heat treatment was followed by X-ray powder diffraction analysis, using a diffractometer equipped with a graphite monochromator (CuK $\alpha$  radiation). For lattice constant calculations, data were collected by step scanning in the range  $10^\circ \leq 2\theta \leq 90^\circ$  with increment of  $0.01^\circ$  ( $2\theta$ ). Bragg angles and peak intensities were determined using a peak analysis computer program taking into account CuK $\alpha_1$  and CuK $\alpha_2$  radiations.

The electron diffraction study was performed with a JEOL 200 CX electron microscope fitted with a side entry goniometer ( $\pm 60^\circ$ ) and the high resolution electron microscopy study with a TOPCON 002 B electron microscope operating at 200 kV.

EDAX measurements were performed with a KEVEX analyzer mounted on the TOPCON electron microscope.

The oxygen content was determined by chemical analysis using iodometric titration.

## Results and Discussion

The EDAX analysis performed on 30 crystals evidenced a constant Bi:Ba ratio of 3 whatever the crystal and whatever the sample. The analysis allows the composition BaBi<sub>3</sub>O<sub>5.5</sub> to be confirmed within the experimental error.

The powder X-ray diffraction (XRD) patterns of three BaBi<sub>3</sub>O<sub>5.5</sub> samples, quenched at 730°C (Fig. 1a), 700°C (Fig. 1b), and 630°C (Fig. 1c), are similar to that of the perovskite BaBiO<sub>3</sub> (Fig. 1d). Nevertheless it is clear from these diffractograms that there exists a structural evolution versus temperature.

The systematic exploration of more than 50 crystals per sample by electron diffraction (E. D.) confirms that there is no secondary phase besides the perovskite-related phases and the crystallization is excellent. No amorphous phase has been detected whatever the synthesis temperature.

The electron diffraction investigation of the 730°C sample shows that all the crystals exhibit the same system of intense reflections corresponding to a cubic subcell close to that of the perovskite BaBiO<sub>3</sub>, i.e.,  $a_p \approx 4.3 \text{ \AA}$ . The reconstruction of the reciprocal lattice confirms that the 730° BaBi<sub>3</sub>O<sub>5.5</sub> exhibits a cubic subcell " $a_p \times a_p \times a_p$ " in agreement with the indexation of main lines of the powder XRD pattern,  $a_p = 4.384 \text{ \AA}$  (Table Ia). However, from this study, it appears clearly that, in contrast to the perovskite BaBiO<sub>3</sub>, this phase does not exhibit a primitive cell but a body-centered cell. This *I*-type symmetry is confirmed from the XRD centered cell (Table Ia) in which the 100 peak is missing. In addition to the intense reflections, the crystals exhibit a system of extra spots whose intensity varies from one to the other. These extra reflections correspond to satellites lying in incommensurate positions along two of the equivalent  $\langle 100 \rangle_p^*$  directions: the  $q$  value of the modulation

TABLE Ia

BaBi<sub>3</sub>O<sub>5.5</sub>: ROOM TEMPERATURE XRD PATTERN FOR SAMPLE ANNEALED AT 730°C (CUBIC SYSTEM  $a = 4.3837$  (7)  $\text{\AA}$ ,  $q = 2.6$ )

$2\theta_{\text{obs}}^a$	$2\theta_{\text{calc}}$	$h$	$k$	$l$	$m$	$n$	$I/I_0$	$d_{\text{calc}}$
20.76	20.775	1	1	0	$\bar{2}$	0	2	4.2742
28.78	28.777	1	1	0	0	0	100	3.0997
41.14	41.150	2	0	0	0	0	24	2.1918
41.85	41.860	1	0	1	2	0	1	2.1563
50.99	50.987	2	1	1	0	0	48	1.7896
59.60	59.603	2	2	0	0	0	16	1.5499
67.48	67.512	3	1	0	0	0	11	1.3862
75.01	74.990	2	2	2	0	0	4	1.2655
82.23	82.213	3	2	1	0	0	18	1.1716

<sup>a</sup> Positions of the lines corresponding to the CuK $\alpha_1$  radiation.

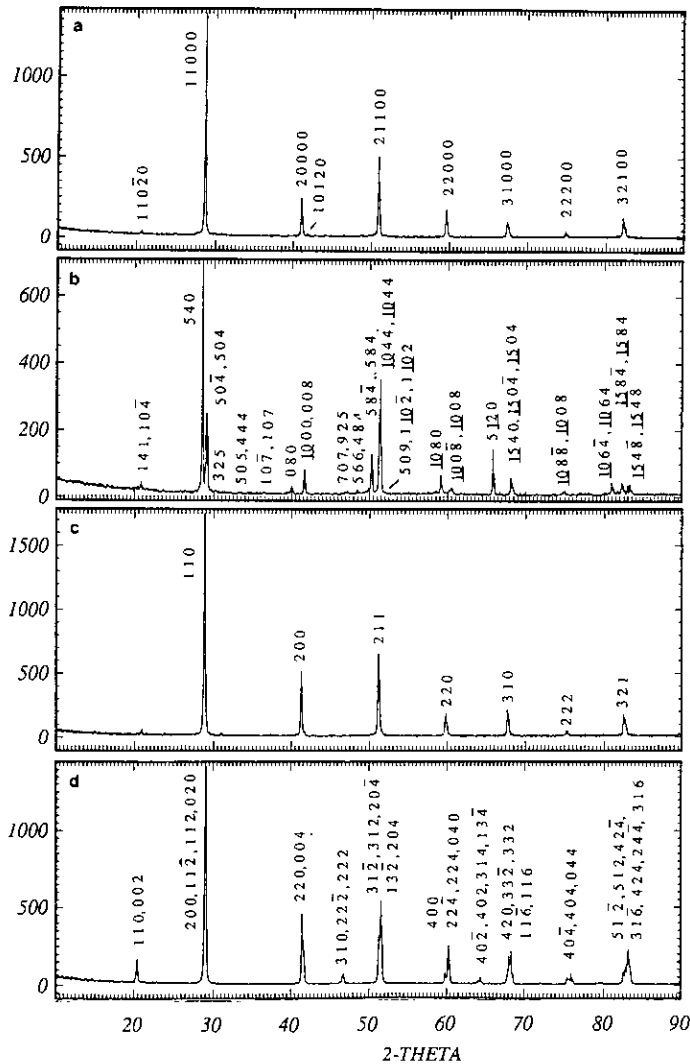


FIG. 1. X-ray powder diffraction patterns (radiation  $\text{CuK}\alpha$ ) for  $\text{BaBi}_3\text{O}_5$  at three temperatures, (a) 730°C, (b) 700°C, (c) 630°C, and for  $\text{BaBiO}_3$  (d).

vector is close to 2.6 and sometimes the intensity of the satellites is strong enough to observe the second order. An example of the [001] pattern is shown in Fig. 2; the reflections are indexed using five indices  $h$ ,  $k$ ,  $l$ ,  $m$ , and  $n$ . The reflection conditions are  $h + k + l + m + n = 2n$ ; a schematic representation of a [001] pattern is drawn in Fig. 2b. It appears that 90° oriented domains are often observed, resulting from the establishment of the modulations along the equiv-

alent directions of the subcell; this is particularly evident on the [111] planes.

The E. D. investigation of the 700°C sample (Fig. 3) shows also that the sample is single phase, but it exhibits a monoclinic distortion of the cubic subcell " $a_p \times a_p \times a_p$ ." These observations allowed the majority of the lines of the powder XRD pattern of this phase to be indexed in a monoclinic subcell (Table Ib) with  $a = 4.328 \text{ \AA}$ ,  $b = 4.497 \text{ \AA}$ ,  $c = 4.328 \text{ \AA}$ ,  $\beta =$

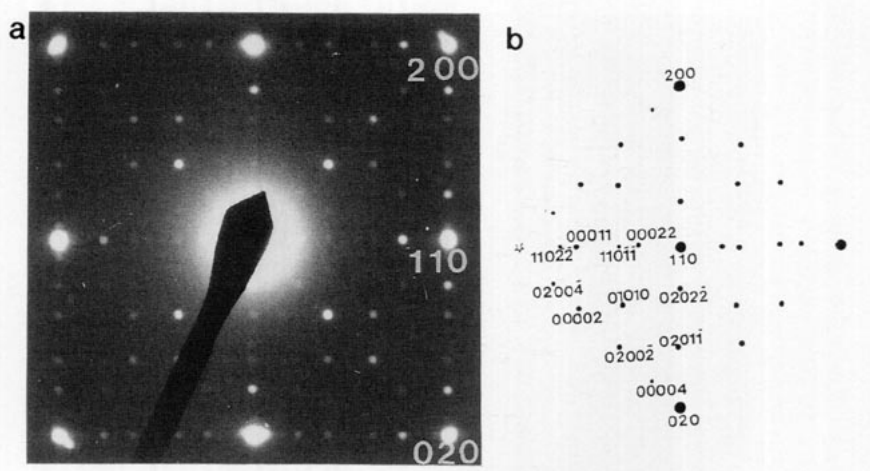


FIG. 2. BaBi<sub>3</sub>O<sub>5.5</sub> at 760°C: (a) [001] electron diffraction patterns. (b) Satellites are indexed using five indices; the indexation is shown in this schematic drawing.

TABLE Ib

BaBi<sub>3</sub>O<sub>5.5</sub>: ROOM TEMPERATURE XRD PATTERN FOR SAMPLE ANEALING AT 700°C ((*h k l*)<sup>\*</sup> REFER TO THE MONOCLINIC SUBCELL *a* = 4.3285 (6) Å, *b* = 4.4968 (5) Å, *c* = 4.3285 (6) Å, β = 90.221 (9)° AND *h k l* REFER TO THE SUPERCELL 5 × *a*, 4 × *b*, 4 × *c*)

$2\theta_{\text{obs}}^a$	$2\theta_{\text{calc}}$	( <i>h k l</i> ) <sup>*</sup>	<i>h k l</i>	$I/I_0^b$	$d_{\text{calc}}$
20.32	20.388		0 4 1	1	4.3524
20.84	20.804		1 4 1	3	4.2662
	20.897		1 0 4		4.2476
28.59	28.601	1 1 0	5 4 0	100	3.1185
29.09	29.095	1 0 1	5 0 4	24	3.0666
29.20	29.210	1 0 1	5 0 4	23	3.0548
30.30	30.323		3 2 5	<1	2.9452
33.22	33.167		5 0 5	1	2.6989
	33.171		4 4 4		2.6986
36.54	36.519		1 0 7	2	2.4585
	36.552		1 0 7		2.4563
40.09	40.070	0 2 0	0 8 0	5	2.2484
41.70	41.700	2 0 0	10 0 0	15	2.1642
			0 0 8		
47.11	47.104		7 0 7	1	1.9259
	47.154		9 2 5		1.9251
48.61	48.596		5 6 6	1	1.8720
	48.625		4 8 4		1.8710
50.30	50.278	1 2 1	5 8 4	23	1.8132
	50.351	1 2 1	5 8 4		1.8108
51.28	51.275	2 1 1	10 4 4	36	1.7803
51.40	51.418	2 1 1	10 4 4	36	1.7757

TABLE Ib—Continued

$2\theta_{\text{obs}}^a$	$2\theta_{\text{calc}}$	( <i>h k l</i> ) <sup>*</sup>	<i>h k l</i>	$I/I_0^b$	$d_{\text{calc}}$
52.02	52.055		5 0 9		1.7554
	52.056		1 10 2	<1	1.7554
	52.063		1 10 2		1.7552
54.42	54.405		3 0 10	<1	1.6850
	54.427		6 6 7		1.6844
58.54	58.519		6 6 8		1.5760
	58.540		3 4 10	2	1.5755
	58.565		9 6 6		1.5749
58.84	58.789		1 0 11	1	1.5694
	58.879		10 6 5		1.5672
59.22	59.210	2 2 0	10 8 0	11	1.5592
60.29	60.315	2 0 2	10 0 8	3	1.5333
60.59	60.573	2 0 2	10 0 8	4	1.5274
65.91	65.891	1 3 0	5 12 0	20	1.4164
68.20	68.207	3 1 0	15 4 0	10	1.3738
68.41	68.404	3 0 1	15 0 4	2	1.3704
68.59	68.584	3 0 1	15 0 4	2	1.3672
74.88	74.901	2 2 2	10 8 8	2	1.2668
75.15	75.133	2 2 2	10 8 8	2	1.2634
81.00	81.020	2 3 1	10 6 4	4	1.1858
81.10	81.133	2 3 1	10 6 4	3	1.1845
82.32	82.339	3 2 1	15 8 4	7	1.1702
82.51	82.508	3 2 1	15 8 4	3	1.1682
83.07	83.061	3 1 2	15 4 8	5	1.1618
83.39	83.399	3 1 2	15 4 8	5	1.1578

<sup>a</sup> See Table Ia.

<sup>b</sup> These values are only given as information; they are altered by the preferred orientation phenomenon.

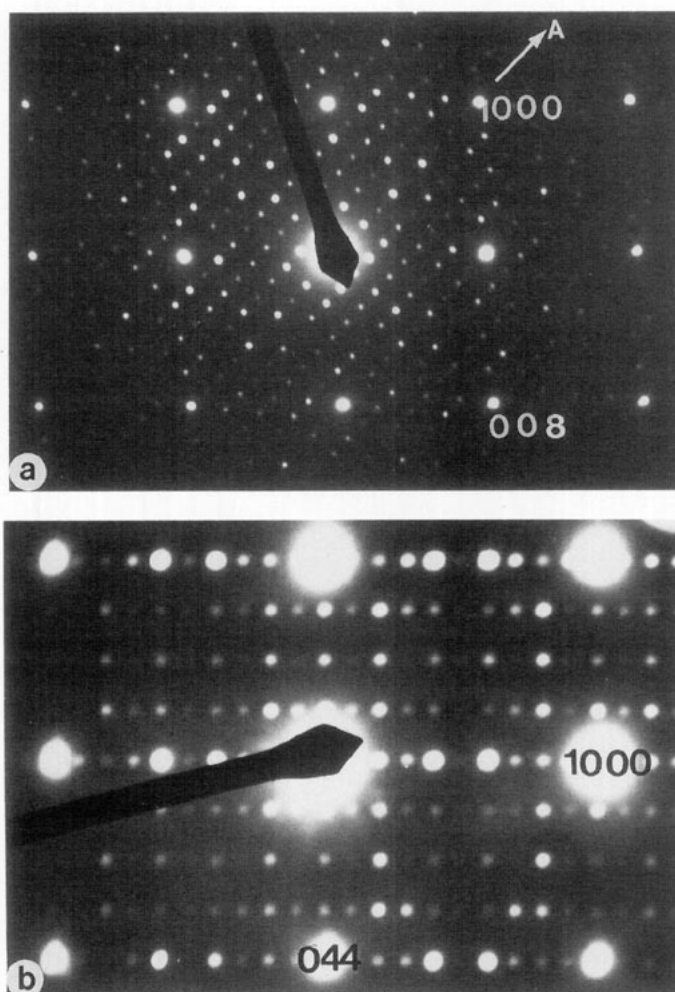


FIG. 3.  $\text{BaBi}_3\text{O}_{5.5}$  at  $700^\circ\text{C}$ : (a)  $[010]$  E.D. pattern; (b)  $[01\bar{1}]$  E.D. pattern.

$90^\circ 22'$ . Again, it is worth pointing out that the subcell of the  $700^\circ\text{C}$   $\text{BaBi}_3\text{O}_{5.5}$  is also body-centered. Moreover, all the crystals exhibit a superstructure, characterized by the actual cell " $5a_p \times 4a_p \times 4a_p$ ." Two typical E. D. patterns,  $[010]$  and  $[01\bar{1}]$ , are shown in Fig. 3a and b, respectively. The high resolution study of this phase showed that the strong variations of contrast due to the superstructure is well established throughout the whole crystal. Unfortunately, the structure is quickly modified under the electron beam so that no significant images were registered.

For the  $630^\circ\text{C}$  sample, three kinds of crystals coexist according to the E.D. observations. The first sort of crystals exhibit a classical cubic cell " $a_p \times a_p \times a_p$ " (Fig. 4a) but without superstructure and satellite spots. The second type of crystals are characterized by a similar cubic cell but with weak incommensurate satellites (Fig. 4b). The third type of crystals are also cubic, but exhibit a doubling of the  $a_p$  parameter; in the latter case the " $2a_p \times 2a_p \times 2a_p$ " cell is characterized by a face centered (F) lattice. On the basis of the E.D. results, the XRD pattern of this sample could be in-

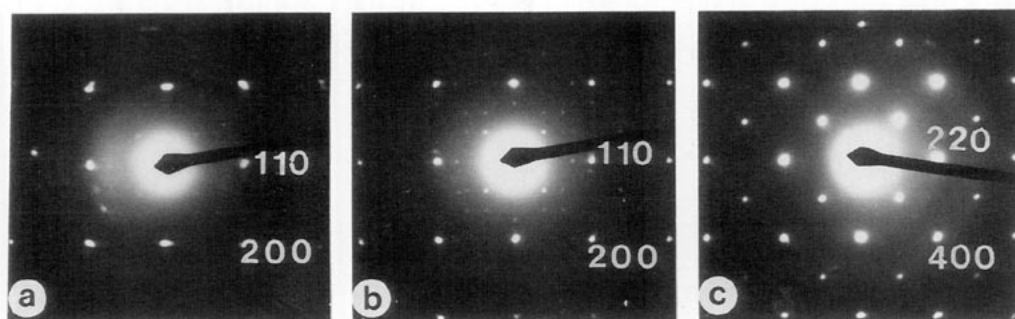


FIG. 4. BaBi<sub>3</sub>O<sub>5.5</sub> at 630°C: [001] E.D. pattern (a) the cell is  $a_p \times a_p \times a_p$ , *I*-type without any extra spots; (b) weak satellites in incommensurate positions are observed; (c) the cell is  $2a_p \times 2a_p \times 2a_p$ , *F*-type lattice.

dexed as a mixture of two cubic phases with  $a = 4.369 \text{ \AA}$  and  $a = 4.375 \text{ \AA}$  respectively (Table Ic).

These results show the existence of a new structural type, BaBi<sub>3</sub>O<sub>5.5</sub>, different from the complex stoichiometric perovskite BaBiO<sub>3</sub> previously studied. Two issues have to be answered dealing with the existence of satellites and of a centered body pseudocubic cell. Order-disorder phenomena on A cationic sites (Ba, Bi) and/or on anionic sites (existence of oxygen vacancies) may

be at the origin of satellites. In spite of the similarity of their XRD patterns with the perovskite, the three different forms of BaBi<sub>3</sub>O<sub>5.5</sub> exhibit E.D. patterns which are not compatible with the perovskite structure; indeed, one observes a body-centered symmetry of the pseudocubic cell, whereas a primitive cell should be detected by E.D. owing to the contribution of oxygen sites. This *I*-type subcell requires that oxygen atoms would be located on both anionic sites  $\frac{1}{2} \frac{1}{2} 0$  and  $\frac{1}{2} 0 0$ , statistically. Taking as a reference the two classical representations of the cubic perovskite (Fig. 5a, b), this suggests that these two types of configurations coexist in the same crystal (Fig. 5c). In the 730°C form the random distribution of such domains would result in an average body-centered cubic cell in which the cationic sites are statistically occupied by barium and bismuth whereas the anionic sites ( $\frac{1}{2} \frac{1}{2} 0$  and  $0 \frac{1}{2}$ ) would be half occupied in a statistical manner by oxygen. Such a model cannot be tested by XRD owing to the too low atom scattering factors of oxygen with respect to barium and bismuth. In this hypothesis, the cells at the junctions between two domains should exist an anion deficiency in order to avoid too short interatomic distances (Fig. 5c); such a feature is in agreement with the chemical formula BaBi<sub>3</sub>O<sub>5.5</sub>□<sub>0.5</sub> and also with the stereoactivity of the 6s<sup>2</sup> lone pair of Bi (III) which tends to extend toward the anionic vacancies. The various forms of

TABLE Ic

BaBi<sub>3</sub>O<sub>5.5</sub>: ROOM TEMPERATURE XRD PATTERN FOR SAMPLE ANNEALED AT 630°C (INDICES REFER TO THE CUBIC SUBCELLS: PHASE 1,  $a = 4.3754 (6) \text{ \AA}$ , PHASE 2,  $a = 4.3690 (20) \text{ \AA}$ )

$hkl_0$	$2\theta_{\text{obs}}^a$	Phase 1			Phase 2		
		$2\theta_{\text{calc}}$	$hkl$	$d_{\text{calc}}$	$2\theta_{\text{calc}}$	$hkl$	$d_{\text{calc}}$
2	20.87 <sup>b</sup>						
100	28.82	28.834	1 1 0	3.0939	28.877	1 1 0	3.0893
1	30.95 <sup>b</sup>						
24	41.25	41.232	2 0 0	2.1877	41.295	2 0 0	2.1845
43	51.12	51.092	2 1 1	1.7862	51.173	2 1 1	1.7836
8	59.73	59.728	2 2 0	1.5469			
7	59.85				59.826	2 2 0	1.5447
7	67.67	67.658	3 1 0	1.3836			
8	67.76				67.772	3 1 0	1.3816
3	75.17	75.158	2 2 2	1.2630			
1	75.34				75.284	2 2 2	1.2612
11	82.42	82.404	3 2 1	1.1694			
5	82.58				82.553	3 2 1	1.1677

<sup>a</sup> See Table Ia.

<sup>b</sup> The lines at  $2\theta = 20.87$  and  $30.95$  can be indexed as satellites with indices  $110\bar{2}0$  and  $110\bar{1}1$ , respectively ( $q = 2.6$ ).

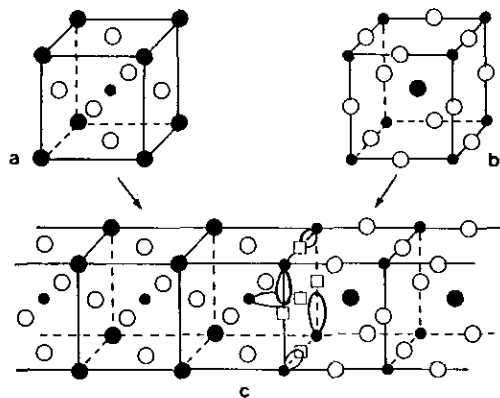


FIG. 5. (a and b) The two classical representations of the perovskite structure. (c) Possible arrangement at the junction of two domains. Small filled circles represent bismuth, large filled circles represent mixed (0.5 Ba, 0.5 Bi) atoms, and open circles represent oxygen.

$\text{BaBi}_3\text{O}_{5.5}$  would differ one from the other by order-disorder phenomena as well as cationic sites as at anionic sites. A neutron diffraction investigation will absolutely be

necessary to understand these new original structures.

## References

1. A. W. SLEIGHT, J. L. GILLSON, AND P. F. BIERSTEDT, *Solid State Commun.* **17**, 27 (1975).
2. R. J. CAVA, B. BATLOGG, J. J., KRAJEWSKI, R. C. FARROW, L. W. RUPP, JR., A. E. WHITE, K. T. SHORT, W. F. PECK, JR., AND T. Y. KOMETANI, *Nature* **332**, 814 (1988).
3. Y. VENEVTSEV, *Mater. Res. Bull.* **6**, 1085 (1971).
4. E. T. SHUVAEVA AND E. G. FESENKO, *Sov. Phys. Crystallogr. Engl. Transl.* **14**, 926 (1970).
5. T. NAKAMURA, S. KOSE, AND T. SATA, *J. Phys. Soc. Jpn.* **31**, 1284 (1971).
6. D. E. COX AND A. W. SLEIGHT, in "Proceedings of the International Conference on Neutron Scattering, Gathinburg" (R. N. Moon, Ed.), Springfield, VA (1976).
7. R. ARPE AND H. K. MÜLLER-BUSCHBAUM, *Z. Anorg. Allg. Chem.* **434**, 73 (1977).
8. D. E. COX AND A. W. SLEIGHT, *Solid State Commun.* **19**, 969 (1976).
9. G. THORNTON AND A. J. JACOBSON, *Acta Crystallogr. Sect. B* **34**, 351 (1978).
10. C. CHAILLOUT, A. SANTORO, J. P. REMEIKA, A. S. COOPER, G. P. ESPINOSA, AND M. MAREZIO, *Solid State Commun.* **65**, 1363 (1988).
11. V. V. SAPONOV, P. KOSTIC, I. KRSTANOVIC, AND M. RISTIC, *Silic. Ind.* **5**, 165 (1990).